

# Fano resonances control and slow light with Bose-Einstein Condensate in a cavity setup

M. Javed Akram,<sup>1,\*</sup> Fazal Ghafoor,<sup>2,†</sup> M. Miskeen Khan,<sup>1,‡</sup> and Farhan Saif<sup>1,§</sup>

<sup>1</sup>*Department of Electronics, Quaid-i-Azam University, 45320 Islamabad, Pakistan.*

<sup>2</sup>*Department of Physics, COMSATS Institute of Information Technology, Islamabad, Pakistan*

We theoretically investigate the probe field transmission in an optomechanical cavity setup with Bose-Einstein Condensate (BEC), where the standing wave that forms in the cavity results in an one-dimensional optical lattice potential. We report that in the presence of atom-atom interactions, the coupling of the cavity field with condensate (Bogoliubov mode), the cavity field fluctuations and the condensate fluctuations leads to the emergence of the tunable Fano resonances in the probe absorption spectrum. Within the experimental reach, based on analytical and numerical simulations, we find that the optomechanical system with BEC provides great flexibility to tune the Fano resonances, as the width of the resonance is controllable by the coupling field and additionally, with the atom-atom interaction. Moreover, Fano resonances are analyzed for the fluctuations of the cavity field and the fluctuations of the condensate with finite atomic two-body interaction, which shows an excellent compatibility with the original Fano resonances as discovered by Ugo Fano. Furthermore, the occurrence of slow light in the probe transmission is explained. It is shown that slow light effect can be enhanced by increasing the atom-atom interaction, It is shown that slow light effect can be enhanced by increasing the atom-atom interaction, which offers a road map towards the realization of on-demand quantum optomechanical memories.

## I. INTRODUCTION

Ugo Fano, in quantum mechanical study of the autoionizing states of atoms [1, 2], discovered that the quantum interference of different transition amplitudes leads to absorption profile which exhibits a minimum or zero. For instance, when a weakly bound state  $|a\rangle$  lies in the continuum  $|E\rangle$ , it has a finite lifetime due to its coupling with the continuum [2–4]. Ugo Fano discovered the effect as resonant and non-resonant processes in photoionization [1, 2]. Since its discovery, the asymmetric Fano resonance has been a characteristic feature of interacting quantum systems, and has been noted spanning a wide range of systems, including quantum dots [5], plasmonic nanoparticles [6], photonic crystals [7], phonon transport, Mach-Zhender-Fano interferometry [2, 10] and electromagnetic metamaterials [8]. Fano resonances are characterized by a steeper dispersion than conventional Lorentzian resonances [2, 6], which make them promising for local refractive index sensing applications [8], to confine light more efficiently [2] and for surface enhanced Raman scattering (SERS) [9]. Besides these applications, Fano resonances have also been used for enhancing the biosensing performance [11, 12], enhanced light transmission [13], slow light [14], and classical analog of electromagnetically induced absorption (EIA) [15]. More recently, Heeg et al. [16] reported that Fano resonances can be used for interferometric phase detection and x-ray quantum state tomography which provides new av-

enues for structure determination and precision metrology [16, 17].

In parallel to these developments in optical science, the field of cavity optomechanics [18, 19] has cemented its place in the present-day photonic technology because of its plethora of promising applications [20, 21]; and serve as basic building block from quantum state-engineering to the quantum communication networks [22–24]. In an optomechanical system (OMS), usually an optical mode couples to mechanical vibrations via radiation pressure induced by circulating optical fields [19]. Due to the ubiquitous nature of the mechanical motion, such resonators couple with many kinds of quantum devices, that range from atomic systems to the solid-state electronic circuits [25–28]. More recently, a new development has been made in the field of levitated optomechanics [29, 30], in which the mechanical oscillator is supported only by the light field. These platforms offer the possibility of a generation of highly-sensitive sensors, which are able to detect (for example) weak forces, with a precision limited only by quantum uncertainties [30].

On the other hand, a variety of other ideas exist for merging cold atom systems with optomechanics [31]. In addition, the optomechanics of both Bose-Einstein condensates [32–38] and degenerate cold atom Fermi gases [39] have been explored theoretically in some depth. Even the Mott insulator to superfluid transition of atoms [40] in an optical lattice coupled to a vibrating mirror has been analyzed, as an example of a strongly interacting quantum system subject to the optomechanical interaction [41]. Fano resonances [42, 43], optomechanically induced transparency [44] with single [45] and multiple windows [43, 46, 47], superluminal and slow light effects [48–56] have also been observed in optomechanical systems, whose nano dimensions and normal environmental conditions have paved the new avenues towards state-

---

\* [mjakram@qau.edu.pk](mailto:mjakram@qau.edu.pk)

† [rishteen@yahoo.com](mailto:rishteen@yahoo.com)

‡ [mmiskeenk16@hotmail.com](mailto:mmiskeenk16@hotmail.com)

§ [farhan.saif@fulbrightmail.org](mailto:farhan.saif@fulbrightmail.org)

of-the-art potential applications, such as imaging and cloaking, telecommunication, interferometry, quantum-optomechanical memory and classical signal processing applications [57–60].

In recent times, interferometric phase detection controlled by Fano resonances and manipulation of slow light propagation have also been reported in the x-ray regime [16, 17]. In this context, the question of interest is how we can control the Fano resonances in optomechanics close to the original Fano profiles leading to sharp and narrow resonances which are of significant importance [2]. In this paper, we give an answer to the question by proposing an interesting scheme to study the tunable Fano resonances in an optical cavity filled with a cigar-shaped Bose-Einstein condensate. We consider the effective Hamiltonian of the system, describing the interaction of the BEC with optical field, as Bose-Hubbard model [40, 61–63]. Unlike previous schemes [42, 43], an advantage of such system is that, additional parameters, namely the atom-atom interaction and condensate fluctuations, provide a coherent control to tune these resonances directly. Moreover, we study the probe field transmission which shows that slow light effect can be enhanced by continuously increasing the atom-atom interaction. This reflects the advantage of our scheme over our earlier schemes [48–56].

The rest of the paper is organized as follows: In Sec. II, we present the system of study and provide detailed model formulation to explain the Fano resonances and slow light effect based on standard input-output theory. Section III is devoted to numerical results and discussions, where the occurrence of tunable Fano profiles have been explained. In Sec. IV, we explain the slow light and its enhancement in the probe transmission. Finally in Sec. V, we conclude our work.

## II. THE MODEL FORMULATION

We consider an optomechanical system with an elongated cigar-shaped Bose-Einstein condensate (BEC) of  $N$  two-level ultracold  $^{87}\text{Rb}$  atoms (in the  $|F=1\rangle$  state) of mass  $m$  and transition frequency  $\omega_a$  of the  $|F=1\rangle \rightarrow |F=2\rangle$  transition of the  $D_2$  line of  $^{87}\text{Rb}$ . Here, both the mirrors are fixed, and the standing wave that circulates in the cavity results in one-dimensional optical lattice potential. The atoms are strongly interacting with the quantized single standing-wave cavity mode of frequency  $\omega_c$ , as shown in Fig. 1. Similar system has been proposed for the quantum state transfer of light fields to the collective density excitations of a Bose-Einstein condensate (BEC) [62]. The system is coherently driven by a strong pump-field of frequency  $\omega_l$  and a weak probe-field with frequencies  $\omega_p$ , respectively. Hence, the optomechanical-Bose-Hubbard (OMBH) Hamiltonian of the system can

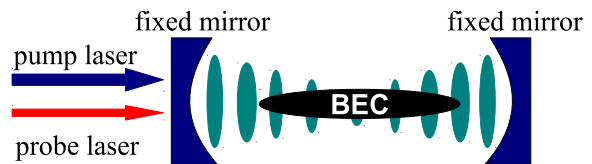


FIG. 1. The schematic representation of the system: an optomechanical system with Bose-Einstein condensate (BEC) confined in an optical cavity with fixed mirrors. A strong driving field of frequency  $\omega_l$  and a weak probe field of frequency  $\omega_p$  are simultaneously injected in the cavity.

be written as [62, 63],

$$H_T = \hbar\Delta_c c^\dagger c + E_0 \sum_j b_j^\dagger b_j + J_0 (\hbar U_0 c^\dagger c + V_{cl}) \sum_j b_j^\dagger b_j + \frac{U}{2} \sum_j b_j^\dagger b_j^\dagger b_j b_j + i\hbar\Omega_l (c^\dagger - c) + i\hbar\varepsilon_p (e^{-i\delta t} c^\dagger - e^{i\delta t} c)$$

In Eq. (1), the first term represents the free Hamiltonian of the single cavity field mode with the creation (annihilation) operator  $c^\dagger$  ( $c$ ). The second term describes the on-site kinetic energy of the condensate with the creation (annihilation) operators  $b_j^\dagger$  ( $b_j$ ) at the  $j$ th site. The third term shows the interaction of the condensate with the cavity field. Here, the parameter  $U_0 = \frac{g_0}{\Delta_a}$  illustrates the optical lattice barrier height per photon and represents the atomic back-action on the field,  $g_0$  is the atom-field coupling and  $V_{cl}$  is the classical potential [63]. The fourth term describes the two-body atom-atom interaction, where  $U$  is the effective on-site atom-atom interaction energy, and  $a_s$  is the two-body  $s$ -wave scattering length as defined above. Finally, the fifth and the sixth terms account for the intense pump laser field and the weak probe laser field, respectively. Here,  $\Omega_l = \sqrt{2\kappa P_l / \hbar\omega_l}$  and  $\varepsilon_p = \sqrt{2\kappa P_p / \hbar\omega_p}$  are amplitudes of the pump and probe fields, respectively, where  $P_l$  ( $P_p$ ) is the power of the pump (probe) field, and  $\kappa$  is the decay rate of the cavity field. Moreover,  $\Delta_c = \omega_c - \omega_l$  and  $\delta = \omega_p - \omega_l$  are the respective detuning of the cavity field and the probe field, with pump field frequency  $\omega_l$ , respectively. Moreover,

$$E_0 = \int d^3x w(\vec{r} - \vec{r}_j) \left( \frac{-\hbar\nabla^2}{2m} \right) w(\vec{r} - \vec{r}_j),$$

$$J_0 = \int d^3x w(\vec{r} - \vec{r}_j) \cos^2(kx) w(\vec{r} - \vec{r}_j),$$

$$U = \frac{4\pi a_s \hbar^2}{m} \int d^3x w|\vec{r}|^4. \quad (2)$$

Here in Eq. (2),  $E_0$  and  $J_0$  describes the effective on-site energies of the condensate, defined in terms of the condensate atomic Wannier functions  $w(\vec{r} - \vec{r}_j)$ , where  $k$  is the wave vector (see appendix for details). For a detailed analysis of the system, we include photon losses in the system and decay rate associated with the condensate mode,  $\kappa$  and  $\gamma_b$ , respectively. Since here we are interested in the mean response of the coupled system to the probe field in the presence of the pump field, we find the expectation values of operators  $c$  and  $X$  respectively,

where  $X = \frac{(b+b^\dagger)}{\sqrt{2}}$  [54]. Based on the Heisenberg equation of motion and the commutation relations  $[c, c^\dagger] = 1$  and  $[b, b^\dagger] = 1$ , the temporal evolutions of  $\langle c \rangle$  and  $\langle X \rangle$  with the mean-field approximation can be written as [45],

$$\begin{aligned} \frac{d\langle c \rangle}{dt} &= -(\kappa + i\Delta)\langle c \rangle - i\sqrt{2}g\langle X \rangle\langle c \rangle + \Omega_l + \varepsilon_p e^{-i\delta t}, \\ \langle \ddot{X} \rangle + \gamma_b \langle \dot{X} \rangle + \omega_b^2 \langle X \rangle &= -2g(\nu + U_{eff})\langle c^\dagger \rangle\langle c \rangle \end{aligned} \quad (3)$$

where  $\Delta = \Delta_c - U_0 N J_0$  is the effective detuning of the cavity field,  $g = U_0 J_0 \sqrt{N} |c_s|^2$ ,  $\omega_b = \sqrt{(\nu + U_{eff})(\nu + 3U_{eff})}$ ,  $U_{eff} = \frac{UN}{\hbar M}$ ,  $\nu = U_0 J_0 |c_s|^2 + \frac{V_{eff} J_0}{\hbar} + \frac{E_0}{\hbar}$ , and  $N$  represents the total number of atoms in  $M$  sites. Since, here we are interested in the mean response of the coupled system to the probe field in the presence of the pump field, we do not include quantum fluctuations which are averaged to zero. This is similar to what has been treated in the context of EIT where one uses atomic mean value equations, and all quantum fluctuations due to both spontaneous emission and collisions are neglected [43, 45]. In order to obtain the steady-state solutions of the above equations, we make the ansatz [64]:

$$\begin{aligned} \langle c \rangle &= c_s + c_- e^{-i\delta t} + c_+ e^{i\delta t}, \\ \langle X \rangle &= X_s + X_- e^{-i\delta t} + X_+ e^{i\delta t}, \end{aligned} \quad (4)$$

where  $c_s$  and  $X_s$  represents the steady-state solutions when  $\varepsilon_p = 0$ . Moreover,  $c_\pm$  and  $X_\pm$  are much smaller than  $c_s$  and  $X_s$  respectively, and are of the same order as  $\varepsilon_p$ . By substituting Eq. (4) into Eqs. (3), respectively, and taking the lowest order in  $\varepsilon_p$  but all orders in  $\Omega_l$ , we get

$$c_s = \frac{\Omega_l}{\kappa + i\Delta}, \quad (5)$$

$$c_- = \frac{[\kappa + i(\Delta - \delta)](\delta^2 - i\delta\gamma_b - \omega_b^2) + ig(\nu + U_{eff})}{[\kappa^2 + \Delta^2 - \delta(\delta + i\kappa)][\delta^2 - i\delta\gamma_b - \omega_b^2] + 2\Delta g(\nu + U_{eff})}, \quad (6)$$

In order to study the optical properties of the output field, we use the standard input-output relation viz. [44],  $c_{out}(t) = c_{in}(t) - \sqrt{2\kappa}c(t)$ . Here,  $c_{in}$  and  $c_{out}$  are the input and output operators, respectively. We can now obtain the expectation value of the output field as,

$$\langle c_{out}(t) \rangle = (\Omega_l - \sqrt{2\kappa}c_s) + (\varepsilon_p - \sqrt{2\kappa}c_-)e^{-i\delta t} - \sqrt{2\kappa}c_+ e^{i\delta t}. \quad (7)$$

Note that, in analogy with Eq. (4), the second term (on right-hand-side) in the above expression corresponds to the output field at probe frequency  $\omega_p$  via the detuning  $\delta = \omega_p - \omega_l$ . Hence, the real and imaginary parts of the amplitude of this term accounts for absorption and dispersion of the whole system to the probe field. Moreover, the transmission of the probe field, which is the ratio of the returned probe field from the coupling system divided by the sent probe field [48], can be obtained as

$$t_p(\omega_p) = \frac{\varepsilon_p - \sqrt{2\kappa}c_-}{\varepsilon_p} = 1 - \frac{\sqrt{2\kappa}c_-}{\varepsilon_p}. \quad (8)$$

For an optomechanical system, in the region of the narrow transparency window, the propagation dynamics of a probe pulse sent to the coupled system greatly alters due to the variation of the complex phase picked up by its different frequency components. The rapid phase dispersion, that is,  $\phi_t(\omega_p) = \arg[t_p(\omega_p)]$ , can cause the transmission group delay given by [19, 48]:

$$\tau_g = \frac{d\phi_t(\omega_p)}{d\omega_p} = \frac{d\{\arg[t_p(\omega_p)]\}}{d\omega_p}. \quad (9)$$

### III. FANO RESONANCES IN THE OUTPUT FIELD

Fano resonances emerge due to the interaction between the cavity field and the Bogoliubov (mechanical) mode of BEC as well as due to the fluctuations of the cavity field and the fluctuations of the condensate with finite atomic two-body interaction. We observe the resonances in the output field at the probe frequency viz.  $E_{out} = \mu + i\nu$ . Here, the real and imaginary parts,  $\mu$  and  $\nu$  respectively, account for the inphase and out of phase quadratures of the output field at probe frequency corresponding to the absorption and dispersion.

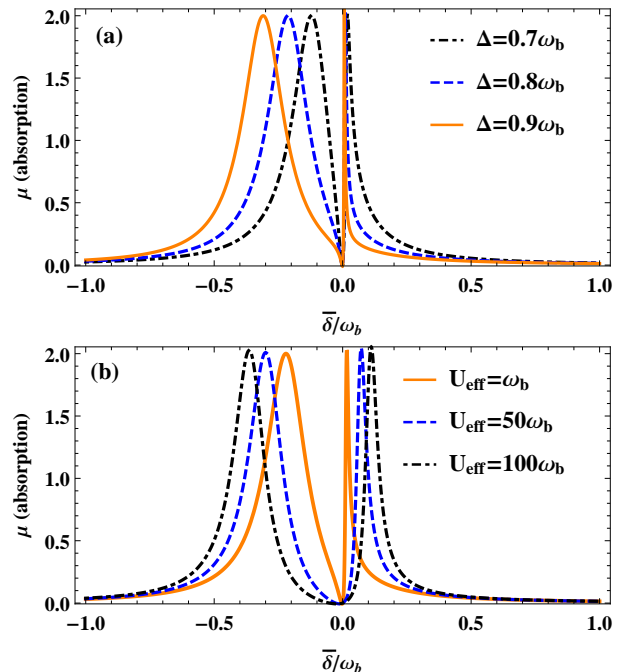


FIG. 2. Fano resonances in the absorption profiles are shown for (a)  $\Delta/\omega_b = 0.7, 0.8, 0.9$  corresponding to dotted, dashed and solid curves respectively, and (b)  $U_{eff}/\omega_b = 1, 50, 100$ , solid, dashed and dotted curves respectively. The rest of the parameters are [33–35]:  $g = 3\omega_b$ ,  $\kappa = 0.1\omega_b$ ,  $U_{eff} = \omega_b$ ,  $\gamma_b/2\pi = 7.5 \times 10^{-3}$  Hz,  $\nu/2\pi = 1000$  KHz,  $\omega_b/2\pi = 10$  KHz.

Since EIT results from the interference of different frequency contributions, it is well known that we can expect

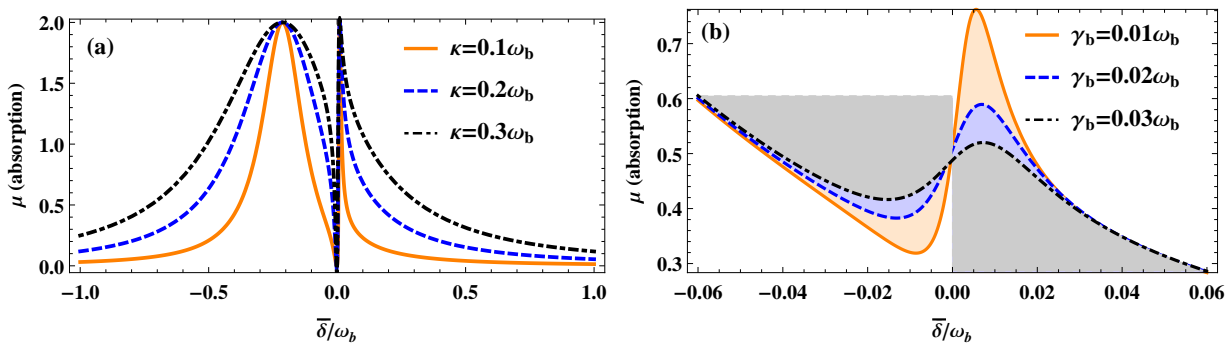


FIG. 3. Fano resonances in the absorption profiles are shown for different values of (a) cavity decay  $\kappa$ , and (b) condensate (Bogoliubov mode) fluctuations  $\gamma_b$ . All the other parameters are same as in Fig. 2.

Fano profiles in EIT under certain conditions [42, 43]. For the resonance region  $\delta \sim \omega_b$ , we analytically obtain the following Fano relation,

$$\mu \approx \frac{2}{1+q^2} \frac{(x+q)^2}{1+x^2}. \quad (10)$$

where  $x = \frac{\nu + U_{eff} - \omega_b}{\Gamma} - q$ ,  $\Gamma = \frac{2\kappa\Delta q}{\kappa^2 + \Omega^2}$ ,  $q = -\Omega/\kappa$ , and  $\Omega = \Delta - \omega_b$ . Note that, the absorption profile in Eq. (10) has the same form as the classic profile of Fano resonance with minimum (zero) at  $x = -q$  and maximum at  $x = 1/q$ . The asymmetry parameter  $q$  is related to the frequency offset  $\Omega$  which controls the emergence of the asymmetric Fano profiles. Physically it means that the anti-Stokes process is not resonant with the cavity frequency [3, 43].

We first discuss the emergence of Fano resonances in the absorption profile with respect to the effective detuning  $\Delta$ . We examine Eqs. (6) and (10), when the coupling laser is detuned from the transition  $\Delta \leftrightarrow \omega_b$ . We present the absorption profiles as a function of normalized detuning  $\bar{\delta}/\omega_b$  ( $\bar{\delta} = \delta - \omega_b$ ) in Fig. 2. We note that when detuning of the cavity field  $\Delta$  is out of resonance with the effective mechanical frequency of the Bogoliubov mode, for instance  $\Delta < \omega_b$ , consequently Fano shapes appear in EIT spectra, in agreement with previous reports [42, 43]. On increasing the detuning  $\Delta$ , the resonance around  $\bar{\delta} \sim \omega_b$  broadens. The line shape has a zero at  $x = -q$ . We note that the interference effects are especially pronounced for small values of  $q$ , i.e. when the maximum and minimum are close to each other. In Fig. 2(b), we examine the effect of finite two-body atom-atom interaction on the Fano profiles. Note that, the narrow Fano profile shown as solid line, goes to the relatively broad resonance as we continuously increase the atom-atom interaction  $U_{eff}$ , in the vicinity of  $\Delta \sim \omega_b$ . The profiles shown in Fig. 2(a) and (b) have common minimum or zero, thus these profiles are Fano resonances [3].

The existence of Fano line shapes in BEC-OMS can be understood by noting that the response of the Bogoliubov mode (BEC) features the narrow spectral width, whereas the cavity modes have orders of magnitude higher spec-

tral width and therefore act as continuum channels. As discussed earlier, the interference of a narrow bound state with a continuum is known to give rise to asymmetric Fano resonances [1, 42, 43]. It is worth noting that EIT occurs when the system meet the resonance condition, that is,  $\Delta = \omega_b$ . However due to the present non-resonant interactions the symmetry of the EIT window is transformed into asymmetric Fano shapes. Moreover, for optomechanical systems in general, we have two coherent processes leading to the building up of the cavity field: (i) the direct building up due to the application of strong pump and weak probe field, and (ii) the building up due to the two successive nonlinear frequency conversion processes between optical mode and a mechanical mode [42, 43]. These two paths contribute in the interference which leads to the emergence of Fano profiles.

For the reason, the cavity decay rate  $\kappa$  and the decay rate of the Bogoliubov mode  $\gamma_b$  effect the Fano resonances. In Fig. 3(a), we indicate that the Fano resonances are sensitive to the cavity decay rate  $\kappa$ . On increasing  $\kappa$ , the resonance around  $\bar{\delta} \sim \omega_b$  becomes narrow. These narrow profiles are of primary significance in precision spectroscopy, metrology and high efficiency x-ray detection [16]. In Fig. 3(b), we show the magnified Fano resonances with effect from the decay rate of the Bogoliubov mode  $\gamma_b$ . Interestingly, we observe a higher maximum, and correspondingly, a lower minimum in the Fano profiles as shown in Fig. 3(b). This effect is analogous to the result in the context of photoionization, in which the value of the minimum depends on the radiative effects [1, 16].

#### IV. SLOW LIGHT IN THE PROBE TRANSMISSION

In this section, we analyze the probe field transmission in BEC-cavity setup, by utilizing the Bose-Hubbard model. Since both the mirrors are fixed, the interaction between the optical mode and the Bogoliubov mode is analogous to the case of single ended cavity [48] which yields normal dispersion in probe phase, that allows the

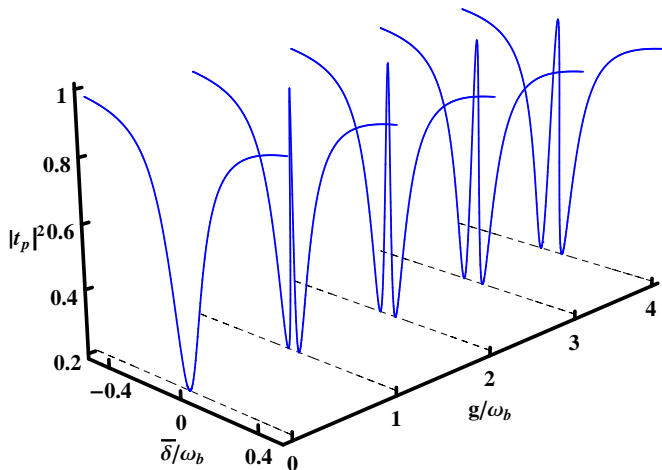


FIG. 4. The transmission  $|t_p|^2$  of the probe field as functions of normalized probe detuning  $\bar{\delta}/\omega_b$  for  $\Delta = \omega_b$  and  $g/\omega_b = 0, 1, 2, 3, 4$  respectively. All the other parameters are the same as in Fig. 2.

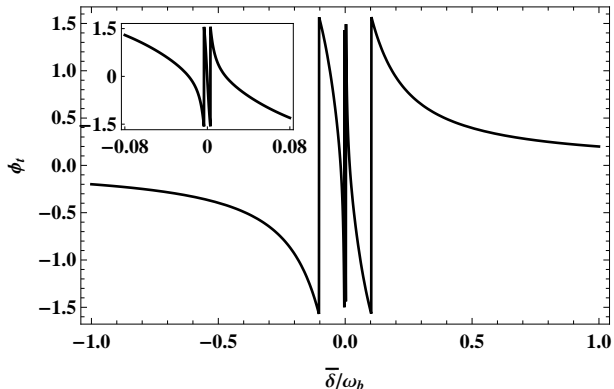


FIG. 5. We plot the phase  $\phi_i$  of the probe field as functions of normalized probe detuning  $\bar{\delta}/\omega_b$  for  $g = \omega_b$ . The inset shows the rapid change around resonance  $\bar{\delta} \sim \omega_b$ . All the other parameters are the same as in Fig. 4.

slow light propagation in the probe transmission. In Fig. 4, we show the transmission  $|t_p|^2$  of the probe field as a function of normalized probe detuning ( $\bar{\delta}/\omega_b$ ), versus the normalized coupling strength  $g/\omega_b$ .

We observe that usual Lorentzian curve appears in the transmission spectrum for  $g = 0$  at  $\bar{\delta} = 0$  ( $\bar{\delta} = \omega_b$ ) in Fig. 4. However, the transparency window occurs in the probe transmission, once the coupling between the cavity field and the condensate mode is present. Figure. 4 depicts that the transparency window in the transmission spectrum broadens and becomes more prominent by continuously increasing the effective coupling strength  $g$ . Interestingly, unlike in traditional optomechanical systems, in addition to the pump laser or the coupling strength, the transparency windows in Fig. 4 can be modulated effectively by the atom-atom interaction.

In Fig. 5, we plot the phase of the probe field versus the

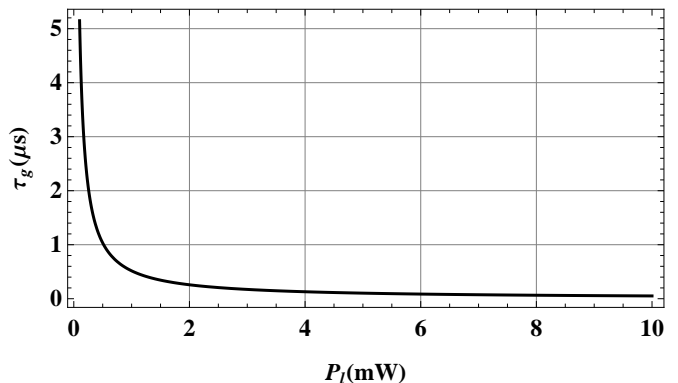


FIG. 6. The group delay  $\tau_g$  versus the pump power  $P_l$  is presented, which shows the pulse delay (subluminal behavior) of the order  $5 \mu\text{s}$  in the probe transmission. All the other parameters are the same as in Fig. 4.

normalized probe detuning for  $\Delta = \omega_b$ . Due to coupling of the cavity field with BEC, the phase of the probe field undergoes a sharp enhancement in the resonant region  $\bar{\delta} \sim \omega_b$ , yielding the rapid phase dispersion [48, 51]. This rapid phase dispersion indicates that group delay of the probe field can be changed significantly through the BEC cavity setup. In Fig. 6, we show group delay  $\tau_g$  versus the pump power  $P_l$ . Since the group delay is positive, which reveals that the characteristics of the transmitted probe field exhibits the slow light effect.

The slow light propagation in the presence of coupling between the optical mode and condensate mode is analogous to the slow light propagation as reported for the mirror-field coupling in traditional optomechanical cavity setup [48]. However, in the former section, we noted that Fano resonances in the probe absorption are significantly altered via atom-atom interaction and also affected by the condensate fluctuations. In order to quantify the effect of atom-atom interaction  $U_{eff}$  and the fluctuations of the condensate mode  $\gamma_b$  on the probe transmission, we present the group delay  $\tau_g$  in Fig. 7 and Fig. 8. Interestingly from Fig. 7, we see that on increasing the atomic two-body interaction ( $U_{eff}$ ), the magnitude of group delay increases. Hence, slow light effect becomes more prominent with large atom-atom interaction. Unlike single-ended optomechanical systems [48] and hybrid atom-cavity systems [51], the delay-bandwidth product in the present case can be greatly enhanced by continuously increasing atom-atom interaction, and may therefore serve as a way to store an optical pulse. This makes our scheme thereby more advantageous for the quantum memory and optical storage applications. Such a BEC cavity-setup has also been realized to transfer the quantum state of light fields to the collective density excitations of BEC [62].

The effect of the condensate fluctuations  $\gamma_b$  on the group delay can be understood from Fig. 8. We see that on increasing  $\gamma_b$ , the magnitude of group delay decreases. This reflects that the lesser the condensate fluctuations

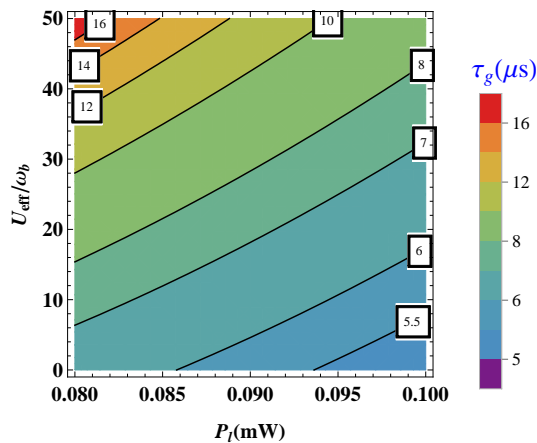


FIG. 7. The group delay  $\tau_g$  versus the pump power  $P_l$  and  $U_{eff}$  is presented. The contour plot shows that pulse delay  $\tau_g$  (subluminal behaviour) can further be enhanced by increasing the atom-atom interaction. All the other parameters are the same as in Fig. 4.

the more obvious we see the slow light effect.

## V. CONCLUSIONS

In conclusion, we have studied Fano resonances, and slow light and its enhancement in a BEC-cavity setup. It is shown that in the presence of atom-atom interactions, the coupling of the cavity field with condensate (Bogoliubov mode), the cavity field fluctuations and the condensate fluctuations leads to the emergence of the tunable Fano resonances in the probe output field. In addition, the occurrence of slow light in the probe transmission is studied, and the group delay is analyzed for the atomic two-body interaction and fluctuations of the condensate. Unlike previous schemes, by utilizing the Bose-Hubbard model in the present setup, we show that the slow light effect can further be enhanced by increasing the atom-atom interaction. This reflects the advantage of our scheme over earlier models [51–56], which pave the way towards achieving longer delays and optical quantum memories. The set of parameters used in our study may help in realizing the characteristics in present-day laboratory experiments.

## APPENDIX

The quite general model many-body Hamiltonian in the second quantized form is given by [63]:

$$H = H_f + H_a \quad (11)$$

Since the BEC-cavity setup is coherently driven by a strong pump-field of frequency  $\omega_l$  and a weak probe-field with frequencies  $\omega_p$ , with amplitudes  $\Omega_l$  and  $\varepsilon_p$ , respectively. Taking the single cavity-field mode into account,

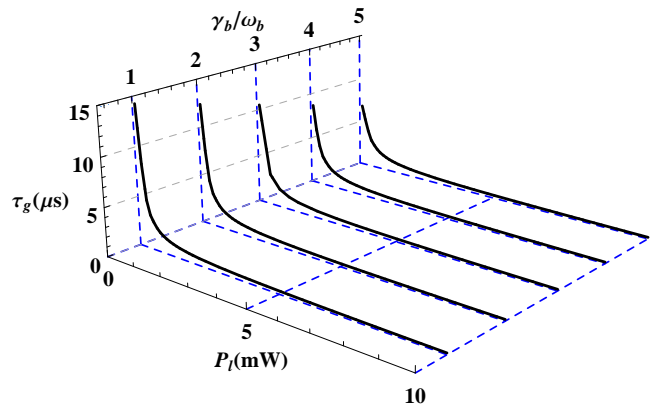


FIG. 8. The group delay  $\tau_g$  versus the pump power  $P_l$  and normalized condensate fluctuations  $\gamma_b/\omega_b$  is presented, which shows that pulse delay (subluminal behaviour) decreases with the increase in the fluctuations of the condensate mode. All the other parameters are the same as in Fig. 4.

the field part in the Hamiltonian (11), i.e.  $H_f$  is given by

$$H_f = \hbar\Delta_c c^\dagger c + i\hbar\Omega_l(c^\dagger - c) + i\hbar\varepsilon_p(e^{-i\delta t}c^\dagger - e^{i\delta t}c) \quad (12)$$

The atom part  $H_a$  is given by

$$H_a = \int d^3x \Psi^\dagger(\vec{r}) H_0 \Psi(\vec{r}) + \frac{2\pi a_s \hbar^2}{m} \int d^3x \Psi^\dagger(\vec{r}) \Psi^\dagger(\vec{r}) \Psi(\vec{r}) \Psi(\vec{r}), \quad (13)$$

where  $\Psi(\vec{r})$  is the field operator for the atoms, and  $a_s$  is the two-body  $s$ -wave scattering length. Moreover,  $H_0$  is the atomic part of the single-particle Hamiltonian  $H_1 = H_f + H_0$ , which in the rotating-wave and dipole approximation has a form:

$$H_0 = \frac{\mathbf{P}^2}{2m} - \hbar\Delta_a \sigma^+ \sigma^- + i\hbar g(x)[\sigma^- c^+ - \sigma^+ c], \quad (14)$$

Here,  $\mathbf{P}$  is the momentum operator of the atom of mass  $m$  and resonance frequency  $\omega_a$ ,  $\sigma^+$ ,  $\sigma^-$ , and  $\sigma_z$  are the raising, lowering, and population difference operators respectively; and  $g(x) = g_0 \cos kx$  is the space dependent atom field coupling. The strong input pump laser field populates the intracavity mode which couples to the atoms through the dipole interaction. The field in turn is modified by the back-action of the atoms. Moreover, the system of study is open as the cavity field is damped by the photon leakage through the coupling mirror with a rate  $\kappa$ . We also consider the system with large detuning, thus spontaneous emission is ignored and hence we can adiabatically eliminate the excited state using Heisenberg equation of motion, which yields the single particle

Hamiltonian:  $H_0 = \frac{\mathbf{p}^2}{2m} + \cos^2 kx[V_{cl} + \hbar U_o c^\dagger c]$ . The parameter  $U_0 = \frac{g_0^2}{\Delta_a}$  is the optical lattice barrier height per photon and represents the atomic backaction on the field. Also  $V_{cl}$  is the external classical potential. The corresponding opto-mechanical-Bose-Hubbard (OMBH) Hamiltonian in Eq. (1) can be obtained by using localized Wannier function  $w(\vec{r} - \vec{r}_j)$  corresponding to  $V_{cl}$ , viz.  $\Psi(\vec{r}) = \sum_j \hat{b}_j w(\vec{r} - \vec{r}_j)$ , where  $\hat{b}_j$  is the correspond-

ing annihilation operator for the bosonic atom at the  $j^{th}$  site.

## ACKNOWLEDGMENTS

We acknowledge HEC for financial support through grant #HEC/20-1374, and Quaid-i-Azam University QAU-URF2014.

- 
- [1] U. Fano, Phys. Rev. **124**, 1866 (1961).  
 [2] A. E. Miroshnichenko, S. Flach, and Y. S. Kivshar, Rev. Mod. Phys. **82**, 2257 (2010).  
 [3] G. S. Agarwal, *Quantum Optics*, (Cambridge University Press, 2013).  
 [4] D.-W. Wang, S.-Y. Zhu, J. Evers, and M. O. Scully, Phys. Rev. A **91**, 011801 (2015). W. Chen, K. Zhang, D. S. Goldbaum, M. Bhattacharya, and P. Meystre, Phys. Rev. A **80**, 011801 (2009).  
 [5] A. C. Johnson, C. M. Marcus, M. P. Hanson, and A. C. Gossard, Phys. Rev. Lett. **93**, 106803 (2004). K. Kobayashi *et al.*, Phys. Rev. B **70**, 035319 (2004). Y. Yoon *et al.*, Phys. Rev. X **2**, 021003 (2012). Kuo-Wei Chen, Yu-Hsin Su, Son-Hsien Chen, Chien-Liang Chen, and Ching-Ray Chang, Phys. Rev. B **88**, 035443 (2013). S. Sasaki, H. Tamura, T. Akazaki, and T. Fujisawa Phys. Rev. Lett. **103**, 266806 (2009).  
 [6] B. Luk'yanchuk *et al.*, Nat. Mater. **9**, 707 (2010). S. Xiao *et al.*, Fortschr. Phys. **61**, 348 (2013).  
 [7] M. V. Rybin, A. B. Khanikaev, M. Inoue, K. B. Samusev, M. J. Steel, G. Yushin, and M. F. Limonov, Phys. Rev. Lett. **103**, 023901 (2009). M. Rahmani *et al.*, Nano Lett. **12**, 2101 (2012). W. Ding, B. Luk'yanchuk, and C. W. Qiu Phys. Rev. A **85**, 025806 (2012). S. Nojima, M. Usuki, M. Yawata, and M. Nakahata Phys. Rev. A **85**, 063818 (2012). Guo Liang Shang, Guang Tao Fei, *et al.*, Sci. Rep. **4**, (2014).  
 [8] N. Verellen *et al.*, Nano Lett. **9**, 1663 (2009). J. Wallauer and M. Walther, Phys. Rev. B **88**, 195118 (2013).  
 [9] J. Ye *et al.*, Nano Lett. **12**, 1660 (2012).  
 [10] A. E. Miroshnichenko, and Y. S. Kivshar, Appl. Phys. Lett. **95**, 121109 (2009).  
 [11] N. Verellen *et al.*, Nano Lett. **11**, 391 (2011).  
 [12] C. Wu *et al.*, Nat. Mater. **11**, 69 (2012).  
 [13] Z. K. Zhou *et al.*, Nano Lett. **11**, 49 (2011).  
 [14] S. Zhang, D. A. Genov, Y. Wang, M. Liu and X. Zhang, Phys. Rev. Lett. **101**, 047401 (2008).  
 [15] R. Taubert, M. Hentschel, J. Kustel and H. Giessen, Nano Lett. **12**, 1367 (2012).  
 [16] K. P. Heeg, C. Ott, D. Schumacher, H.-C. Wille, R. Rohlsberger, T. Pfeifer, and J. Evers, Phys. Rev. Lett. **114**, 207401 (2015).  
 [17] K. P. Heeg, J. Haber, D. Schumacher, L. Bocklage, H.-C. Wille, K. S. Schulze, R. Loetzsch, I. Uschmann, G. G. Paulus, R. Ruffer, R. Rohlsberger, and J. Evers, Phys. Rev. Lett. **114**, 203601 (2015).  
 [18] P. Meystre, Ann. Phys. (Berlin) **525**, 215 (2013).  
 [19] M. Aspelmeyer, T. J. Kippenberg, F. Marquardt, Rev. Mod. Phys. **86**, 1391 (2014).  
 [20] B. Rogers, N. Lo Gullo, G. De Chiara, G. M. Palma, and M. Paternostro, Quantum Meas. Quantum Metrol. **2**, 11 (2014).  
 [21] G. Kurizki, P. Bertet, Y. Kubo, K. Mølmer, D. Petrosyan, P. Rabl, and J. Schmiedmayer, PNAS **112**, 3866 (2015).  
 [22] H. J. Kimble, Nature **453**, 1023-1030 (2008).  
 [23] J. I. Cirac, and P. Zoller, Nature **404**, 579 (2000).  
 [24] T. D. Ladd *et al.* Nature **464**, 45 (2010).  
 [25] L. Tian, Ann. Phys. (Berlin) **527**, 1 (2015).  
 [26] L. Tian, and P. Zoller, Phys. Rev. Lett. **93**, 266403 (2004).  
 [27] W. K. Hensinger *et al.*, Phys. Rev. A **72**, 041405(R) (2005).  
 [28] M. J. Akram, K. Naseer, and F. Saif, arXiv preprint arXiv:1503.01951 (2015).  
 [29] T. S. Monteiro, J. Millen, G. A. T. Pender, F. Marquardt, D. Chang, and P. F. Barker, New J. Phys **15**, 015001 (2013).  
 [30] G. A. T. Pender, P. F. Barker, Florian Marquardt, J. Millen, and T. S. Monteiro, Phys. Rev. A **85**, 021802 (2012). J. Millen, P. Z. G. Fonseca, T. Mavrogordatos, T. S. Monteiro, and P. F. Barker, Phys. Rev. Lett. **114**, 123602 (2015).  
 [31] D. Hunger, S. Camerer, M. Korppi, A. Jockel, T. W. Hansch, and P. Treutlein, C. R. Phys. **12**, 871 (2011).  
 [32] S. Martelucci, A. N. Chester, A. Aspect, and M. Inguscio, *Bose-Einstein Condensation and Atom Lasers*, New York: Kluwer academic publisher (2002).  
 [33] F. Brennecke, S. Ritter, T. Donner, and T. Esslinger, Science **322**, 235 (2008).  
 [34] K. W. Murch *et al.*, Nat. Phys. **4**, 561 (2008).  
 [35] A. Schliesser *et al.*, Nat. Phys. **4**, 415 (2008).  
 [36] W. Chen, D. S. Goldbaum, M. Bhattacharya, and P. Meystre, Phys. Rev. A **81**, 053833 (2010).  
 [37] H. D. Jing, D. S. Goldbaum, L. Buchmann, and P. Meystre, Phys. Rev. Lett. **106**, 223601 (2011).  
 [38] S. K. Steinke, S. Singh, M. E. Tasgin, P. Meystre, K. C. Schwab, and M. Vengalattore, Phys. Rev. A **84**, 023841 (2011).  
 [39] P. Kanamoto and P. Meystre Phys. Rev. Lett. **104**, 063601 (2010). M. Asjad, M. A. Shahzad, and F. Saif, Eur. Phys. J. D **67**, 198 (2013). S. Yang, M. Al-Amri, and M. S. Zubairy, J. Phys. B: At. Mol. Opt. Phys. **47** 135503 (2014).  
 [40] C. E. Creffield and T. S. Monteiro, Phys. Rev. Lett. **96**, 210403 (2006).  
 [41] J. Larson, Damski, G. Morigi, and M. Lewenstein, Phys. Rev. Lett. **100**, 050401 (2008).

- [42] K. Qu and G. S. Agarwal, Phys. Rev. A **87**, 063813 (2013).
- [43] M. J. Akram, F. Ghafoor, and F. Saif, J. Phys. B: At. Mol. Opt. Phys. **48**, 065502 (2015).
- [44] S. Weis, R. Rivière, S. Deléglise, E. Gavartin, O. Arcizet, A. Schliesser, and T. J. Kippenberg, Science **330**, 1520 (2010).
- [45] G. S. Agarwal and S. Huang, Phys. Rev. A **81**, 041803(R) (2010).
- [46] H. Wang, X. Gu, Y. X. Liu, A. Miranowicz, and F. Nori, Phys. Rev. A **90**, 023817 (2014).
- [47] F. Ghafoor, Laser Phys. **24**, 035702 (2014). M. J. Akram, F. Ghafoor, and F. Saif, Multiple electromagnetically induced transparency, slow and fast light in hybrid optomechanics (to be published).
- [48] A. H. Safavi-Naeini, T. P. Alegre, J. Chan, M. Eichenfield, M. Winger, Q. Lin, J. T. Hill, D. E. Chang, and O. Painter, Nature (London) **472**, 69 (2011).
- [49] J. D. Teufel, D. Li, M. S. Allman, K. Cicak, A. J. Sirois, J. D. Whittaker, and R. W. Simmonds, Nature **471**, 204 (2011).
- [50] M. D. Stenner, D. J. Gauthier and M. A. Niefeld, Nature **425**, 695 (2003).
- [51] M. J. Akram, M. M. Khan and F. Saif, Phys. Rev. A **92**, 023846 (2011).
- [52] D. Tarhan, Act. Phys. Pol. A **124**, 46 (2013).
- [53] D. Tarhan, S. Huang, and O. E. Mustecaplioglu, Phys. Rev. A **87**, 013824 (2013).
- [54] B. Chen, C. Jiang, and K. D. Zhu, Phys. Rev. A **83**, 055803 (2011).
- [55] X-G Zhan *et al.*, J. Phys. B: At. Mol. Opt. Phys. **46**, 025501 (2013).
- [56] C. Jiang, H. Liu, Y. Cui, X. Li, G. Chen, and B. Chen, Opt. Express **21**, 12165 (2013).
- [57] R. W. Boyd and D. J. Gauthier, Progress in Optics 43, edited by E. Wolf, Chap. 6, p. 497. (Elsevier, Amsterdam, 2002).
- [58] D. E. Chang, A. H. Safavi-Naeini, M. Hafezi, and O. Painter, New J. Phys **13**, 023003 (2011).
- [59] P. W. Milonni, *Fast light, slow light and lefthanded light* (Institute of Physics Publishing, Bristol, 2005).
- [60] F. Ghafoor, B. A. Bacha, and S. Khan, Phys. Rev. A **91**, 053807 (2015).
- [61] A. B. Bhattacharjee, Phys. Rev. A **80**, 043607 (2009). A. Bhattacharjee, Opt. Commun. **281**, 3004 (2008).
- [62] T. Kumar, A. B. Bhattacharjee, P. Verma, and ManMohan, J. Phys. B: At. Mol. Opt. Phys. **44**, 065302 (2011).
- [63] I. B. Mekhov, and H. Ritsch, J. Phys. B: At. Mol. Opt. Phys. **45**, 102001 (2012).
- [64] R. W. Boyd, *Nonlinear Optics*, Academic Press, New York, (2010).